Machine learning based image analysis for the automated counting of motor neurons in a live cell screening system without the use of specialized fluorescent probes

Samuel V. Alworth[1], André Blumenstein[2,3], Anthony C. Arvanites[2,3], Justin Ichida[2,3], Chieko Nakad
Yasujiro Kiyota[4], Kevin Eggan[2,3], Lee L Rubin[2,3], James S.J. Lee[1]

[1]DRVision Technologies LLC, Bellevue WA 98008; [2]Harvard Stem Cell Institute, Harvard University, Cambridge, MA 02138; [3]Department of Stem Cell and Regenerative Biology, Harvard University, Cambridge, MA 02138; [4]Nikon Corporation, Yokohama Kanagawa Prefecture, 244-8533 Japan

Introduction

Using transcription factor mediated direct conversion of fibroblasts into different cell types is becoming a popular method for the high-throughput construction of patient-specific disease models. Using these models for certain applications, such as phenotypic screening, is dependent on the ability to readily recognize the cellular phenotypes of interest, such as the successfully differentiated cells. This is often achieved using a lentiviral vector to deliver a differentiation-activated fluorescent reporter. We have produced multiple lines of spinal cord motor neurons using a set of 6 transcription factors (Son et al., Cell Stem Cell, 2011, 9:205) and a lentiviral Hb9::RFP reporter. However, the reporter is non-specific, there can be background expression of RFP in cells other than motor neurons. Furthermore, it is advantageous to accurately define motor neurons on the basis of subtle structural features, such as the presence of neurites. Here we report our validation of an innovative image analysis recipe (processing routine) using CL-Quant image analysis software (Nikon Corporation). The recipe incorporates two levels of machine learning. The first is done at the image processing level to enhance the fine neuronal processes, making use of a teachable machine learning method called soft matching. And the second is done at the feature classification level, creating motor neuron classifiers from the cell measurements and uses a teachable machine learning method called regulated decision trees. The method successfully automates counting and generates correct results in the validation data.

Assay Overview

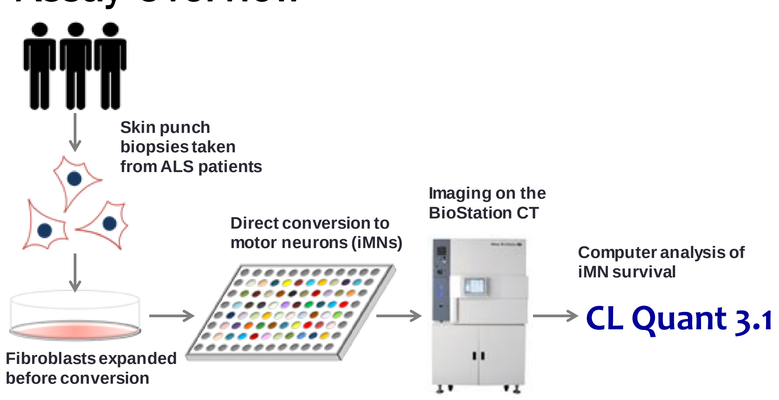

Figure 1. Induced motor neuron (iMN) generation, imaging and automated scoring

Assay overview for patient specific induced motor neuron survival assay. Patient skin biopsies are expanded, placed into 96 well plates, and undergo transcription mediated direct conversion to motor neurons. Experiments are carried out on the BioStation CT, which provides continuous incubation and imaging of the cells every 6 hours for 48 hours. A recipe was created in CL-Quant to automate the counting of motor neurons at every time point.

Challenges for Image Analysis

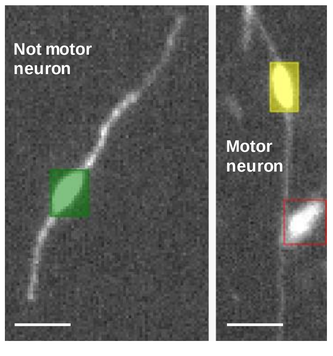

Figure 2. Illustration of cell type morphologies

The lack of a high specificity motor neuron reporter poses a challenge for image analysis. The high throughput 96 well plate format provides low signal to noise (S/N) making it more difficult to accurately detect fine cellular structures – especially the neuronal processes which are important for classification. The classification of subtle morphological differences is also a challenge. A good pattern recognition framework is needed in addition to good image processing functions. White scale bars = 40 μm.

Teachable Image Analysis in CL-Quant

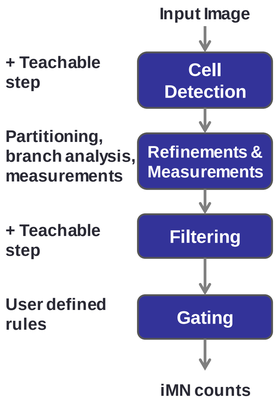

Figure 3. Image analysis processing flow

Each processing step is implemented in CL-Quant procedures which are combined into a CL-Quant recipe that can be batch applied to multiple images. Cell detection step identifies cell regions and fine neuronal processes. Refinements and measurements step performs morphometric analysis, such as distinguishing individual cells, cell bodies and processes and analysis of arbor lengths and branches and the quantification of them. A filtering step is done to remove non iMN detections. Gating rules are created by expert users during recipe creation to encode their selection criteria. Two types of machine learning technologies are used.

Figure 4. Teaching a detection procedure

(A) An example image. (B) The robust pattern matching (called Soft Matching) generates a confidence image (F) greatly improving S/N of neuronal processes (green arrow) over traditional methods such as noise correction and edge enhancements (E) yielding detection result (G). Threshold overlay (D) illustrates the lack of connectivity of the processes in the original image (C).

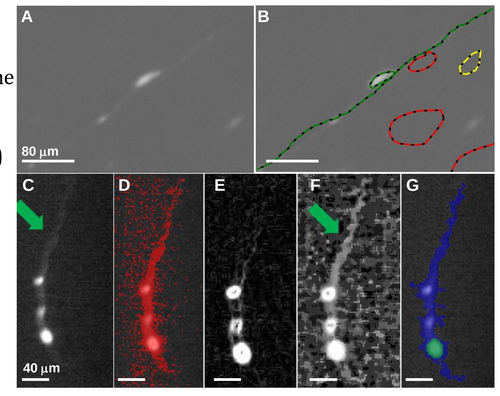

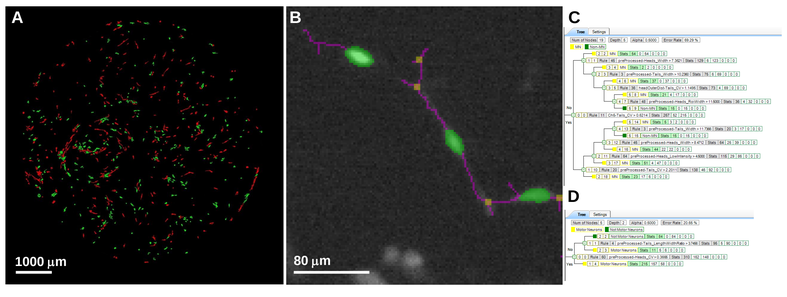

Figure 5. Teaching a filtering procedure

Obvious non iMN cells can be removed by decision procedures. A) Shows the result of the filter step, red color shows cells which are removed. B) Illustrates fine structural detection (i.e. cell body vs. processes; branch points shown as squared) which are quantified and used for classification. C-D) show the decision trees automatically created by CL-Quant based on our teaching. Nodes in the trees can be pruned and re-assigned so that no iMNs are removed. In the teaching data, 31.4% of non iMNs (114 of 363 non iMN cells used for teaching) were removed yet no iMNs are removed (perfect sensitivity).

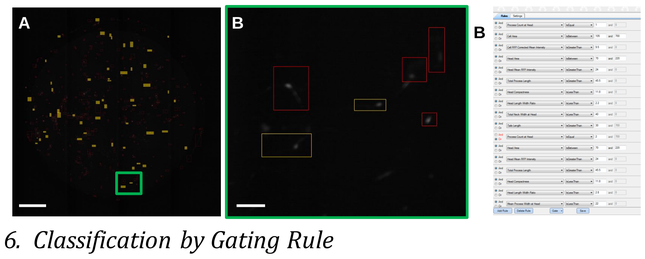

Figure 6. Classification by Gating Rule

Lastly, trained scientists encoded their own criteria for iMN classification using gating rules. Different criteria are used if the cell has 1, 2 or > 2 processes. A) Shows the final result after gating. B) Shows expanded region from A in green square. iMNs are highlighted with yellow region after classification. C) Shows the CL-Quant gating rule construction software interface. White bars = 1000 μm.

Validation

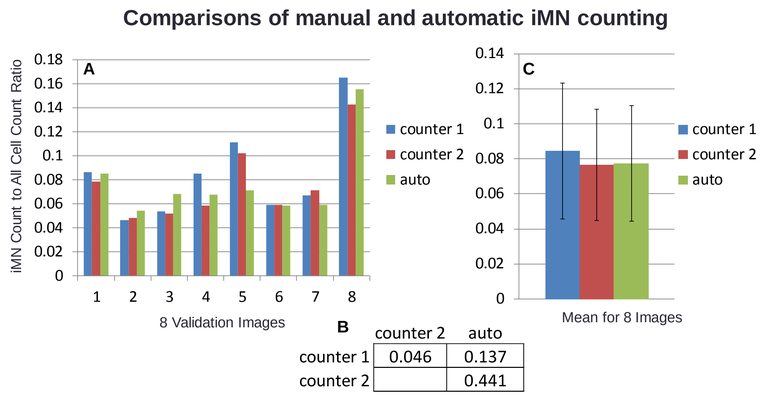

Figure 7. Validation through comparison with manual counting

Validation is performed through comparison with manual counting. The proportion of motor neurons to all cells initially detected by the recipe is reported. The independent counts of two expert scientists and the recipe's final motor neuron ratios are compared on eight validation images. A) shows that the counts of the two human and recipe (auto) have similar trend. B) P-values for paired students' T test comparing the three counters shows less difference between the automatic counting and each of the human counters than there is between human counters . C) Mean values of the count ratios across all eight images show clearly that automatic counting is similar to human counting (error bars show +/- one standard deviation).

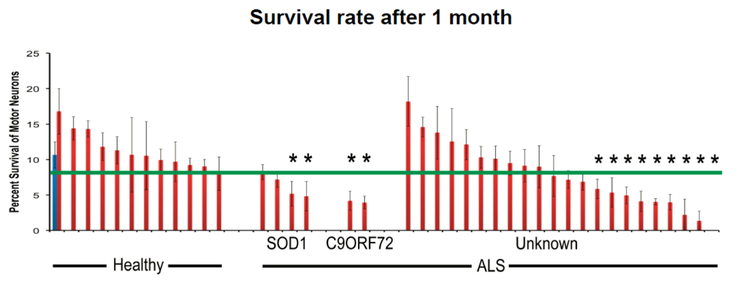

Figure 8. Validation in a preliminary patient study

The recipe was evaluated in a pilot assay of motor neuron survival in sixty ALS patients *in vitro*. 60 well plates of images were analyzed by CL-Quant recipe. The experiment confirms that iMNs from many patients exhibit rapid degeneration. Blue bar is the average survival of control iMNs. The results show that the recipe is able to generate expected motor neuron counts (i.e. comparing healthy and diseased) in a high throughput analysis.

Conclusion

For the screening of patient-specific disease models it is prohibitively expensive and impractical to tailor highly specific genetic reporters for each patient line. Though the HB9::RFP reporter does label cells other than motor neurons, it is possible for skilled scientists, knowledgeable in motor neuron morphology, to manually count the motor neurons. However, this is tedious, the criteria for selection are non-standardized and it is not practical for high volume studies. In the current study, we have used the teachable CL-Quant software to create a powerful recipe that can score motor neurons on par with human operators. It makes use of two of CL-Quant's innovative machine learning technologies. We have used it in a preliminary patient specific study of ALS and healthy patients, and the recipe reliably scores the motor neuron survival phenotype showing healthy patients having greater motor neuron survival than ALS patients.

Acknowledgements

The project described was supported in part by Grant Number R44HL106863 from the National Heart, Lung and Blood Institute. The content is solely the responsibility of the authors and does not necessarily represent the official views of the National Heart, Lung and Blood Institute.